Evidence for van der Waals adhesion in gecko seta

Kellar Autumn[†‡], Metin Sitti[§], Yiching A. Liang[¶], Anne M. Peattie[†‖], Wendy R. Hansen[†], Simon Sponberg[†], Thomas W. Kenny[¶], Ronald Fearing[§], Jacob N. Israelachvili[**], and Robert J. Full[††]

[†]Department of Biology, Lewis & Clark College, Portland, OR 97219; Departments of [§]Electrical Engineering and Computer Science, and [††]Integrative Biology, University of California, Berkeley, CA 94720; [¶]Department of Mechanical Engineering, Stanford University, Stanford, CA 94305; and [**]Department of Chemical Engineering, University of California, Santa Barbara, CA 93105

Edited by Thomas Eisner, Cornell University, Ithaca, NY, and approved July 9, 2002 (received for review April 29, 2002)

Geckos have evolved one of the most versatile and effective adhesives known. The mechanism of dry adhesion in the millions of setae on the toes of geckos has been the focus of scientific study for over a century. We provide the first direct experimental evidence for dry adhesion of gecko setae by van der Waals forces, and reject the use of mechanisms relying on high surface polarity, including capillary adhesion. The toes of live Tokay geckos were highly hydrophobic, and adhered equally well to strongly hydrophobic and strongly hydrophilic, polarizable surfaces. Adhesion of a single isolated gecko seta was equally effective on the hydrophobic and hydrophilic surfaces of a microelectro-mechanical systems force sensor. A van der Waals mechanism implies that the remarkable adhesive properties of gecko setae are merely a result of the size and shape of the tips, and are not strongly affected by surface chemistry. Theory predicts greater adhesive forces simply from subdividing setae to increase surface density, and suggests a possible design principle underlying the repeated, convergent evolution of dry adhesive microstructures in gecko, anoles, skinks, and insects. Estimates using a standard adhesion model and our measured forces come remarkably close to predicting the tip size of Tokay gecko seta. We verified the dependence on size and not surface type by using physical models of setal tips nanofabricated from two different materials. Both artificial setal tips stuck as predicted and provide a path to manufacturing the first dry, adhesive microstructures.

In the 4th century B.C., Aristotle observed the ability of the gecko to "run up and down a tree in any way, even with the head downwards" (1). Two millennia later, we are uncovering the secrets of how geckos use millions of tiny foot-hairs to adhere to even molecularly smooth surfaces. We tested the two currently competing hypotheses (2, 3) of adhesion mechanisms in gecko setae: (*i*) thin-film capillary forces (or other mechanisms relying on hydrophilicity) and (*ii*) van der Waals forces. First, we tested the capillary and van der Waals hypotheses experimentally. Second, we used our experimentally measured adhesion forces in a mathematical model (4) to generate an independent prediction of the size of a setal tip. We compared the predicted size with the empirical values measured by electron microscopy (5). Third, we fabricated a physical model of gecko setal tips from two different materials. We then compared the adhesive function of the physical model to predicted force values from the mathematical model.

Previously, we showed by calculation that our direct force measurements of a single gecko seta (3) were consistent with adhesion by van der Waals forces, but we could not reject the only other untested mechanism—wet, capillary adhesion that relies on the hydrophilic nature of the surface. Capillary forces contribute to adhesion in many insects (6–13), frogs (14–16), and even some mammals (17). Unlike many insects, geckos lack glands on the surfaces of their feet (18–20). However, this does not preclude the role of thin film capillary adhesion (2, 21) caused by the adsorption or capillary condensation of water from the atmosphere, because even a monolayer of water molecules can cause significant capillary attraction between hydrophilic surfaces (22, 23). Hydrophilic surfaces have low water contact angle (θ) and hydrophobic surfaces have high θ. The first studies to provide direct evidence for intermolecular forces in gecko setae (24, 25) are consistent with the use of capillary adhesion (2), and suggest that the strength of setal adhesion may be correlated with the hydrophilicity of the surface as measured by the water contact angle (θ).

However, measuring setal forces on surfaces that vary in water contact angle (θ) (24, 25) cannot distinguish wet, capillary adhesion from van der Waals dispersion force. In the case of two identical solid surfaces, the adhesion energy (W) between them is related to the contact angle (θ) of a liquid droplet on one of the surfaces by means of the Young–Dupre' equation, $\gamma_L(1 + \cos\theta) = W$, where γ_L is the surface tension (or energy) of the liquid (L) in units of mN/m (or mJ/m^2). However, if the two adhering surfaces are of different materials, as for gecko setae (G) on a substrate surface (S) in Hiller's experiments (24, 25), the adhesion energy (W_{GS}) bears no simple relation to the liquid (water) contact angle (θ) on either surface (23), and thus cannot be used to draw conclusions about van der Waals force. van der Waals dispersion force is strong between polarizable surfaces, and is only weakly dependent on the hydrophobicity of the interacting surfaces (23). Previous studies found that geckos fail to adhere to hydrophobic, weakly polarizable surfaces [polytetrafluoroethylene where $\theta = 105°$ (25), and the dielectric constant, $\varepsilon = 2.0$ (23)], but the low adhesion could be caused by reduced capillary adhesion, reduced van der Waals force, or both.

To test directly whether capillary adhesion or van der Waals dispersion force is the primary mechanism of adhesion in geckos, we separated polarizability from polarity (hydrophobicity and hydrophilicity) by measuring adhesion on two polarizable semiconductor surfaces that varied greatly in hydrophobicity. We measured the parallel force of single gecko toes on a gallium arsenide (GaAs) semiconductor surface that is highly hydrophobic ($\theta = 110°$), but highly polarizable ($\varepsilon = 10.88$; ref. 26). As a control, we measured parallel force on the strongly hydrophilic ($\theta = 0°$) and polarizable ($\varepsilon > 4.5$; ref. 23) silicon dioxide (SiO_2) semiconductor surface. We also compared the perpendicular force of single isolated gecko setae on hydrophilic (SiO_2, $\theta = 0°$) and hydrophobic (Si, $\theta = 81.9°$) microelectromechanical systems (MEMS) force sensors. If wet, capillary adhesive forces dominate, we expect a lack of adhesion on the strongly hydrophobic GaAs and Si MEMS surfaces. In contrast, if van der Waals forces dominate, we predict large adhesive forces on the hydrophobic, but polarizable GaAs and Si MEMS surfaces. In either case we expect strong adhesion to the hydrophilic SiO_2 semiconductor and MEMS control surfaces (Fig. 1).

If van der Waals force is the principle mechanism of adhesion in gecko setae, then adhesive force should depend more on size of the setal tips (spatulae) than on the nature of the setal

This paper was submitted directly (Track II) to the PNAS office.

Abbreviations: GaAs, gallium arsenide; MEMS, microelectromechanical systems; AFM, atomic force microscope; PDMS, polydimethylsiloxane.

[‡]To whom reprint requests should be addressed. E-mail: autumn@lclark.edu.

[‖]Present address: Department of Integrative Biology, University of California, Berkeley, CA 94720.

www.pnas.org/cgi/doi/10.1073/pnas.192252799

Downloaded from https://www.pnas.org by CENTRAL SOUTH UNIVERSITY on November 9, 2026 from IP address 218.76.28.177.

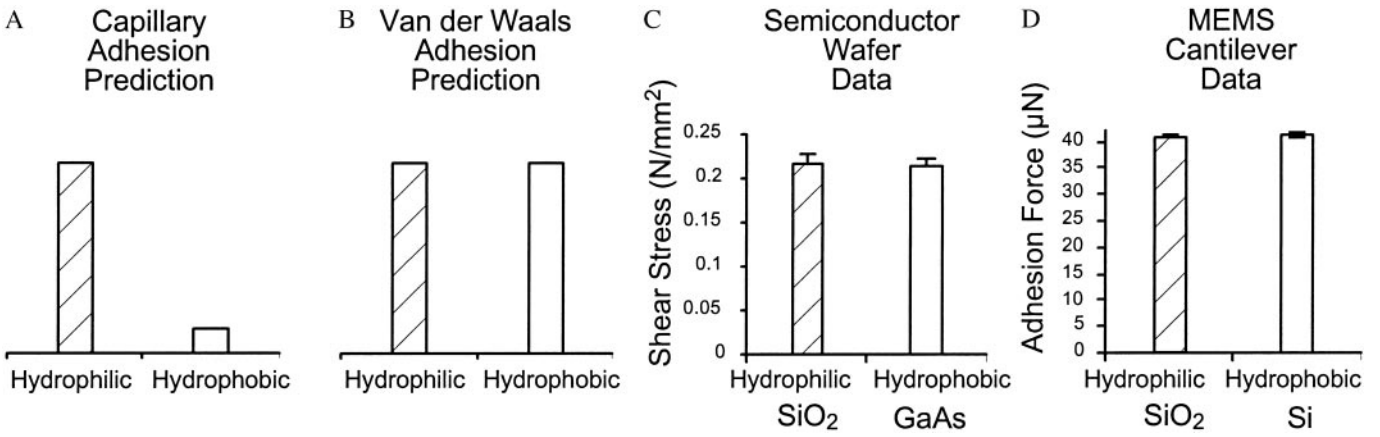


Fig. 1. Force of gecko setae on highly polarizable surfaces versus for surface hydrophobicity. (*A*) Wet adhesion prediction. (*B*) van der Waals prediction. (*C*) Results from toe on highly polarizable semiconductor wafer surfaces differing in hydrophobicity. (*D*) Results from single seta attaching to highly polarizable MEMS cantilevers differing in hydrophobicity. Note that geckos fail to adhere to hydrophobic, weakly polarizable surfaces [polytetrafluoroethylene where θ = 105° (25) and the dielectric constant, ε = 2.0 (23)]. Adhesion to hydrophilic and hydrophobic polarizable surfaces was similar. Therefore, we reject the hypothesis that wet, capillary interactions are necessary for gecko adhesion in favor of the van der Waals hypothesis.

material (23). This theoretical dependence on size and not surface type encouraged our nanofabrication of synthetic spatulae. If van der Waals forces are responsible for gecko adhesion, then we should be able to fabricate physical models of spatulae whose surfaces differ in material, but are equally effective in adhesion.

Materials and Methods

Foot Adhesion. *Hydrophobic and hydrophilic semiconductor wafers.* We placed a single toe of nine live Tokay geckos (*Gekko gecko*) against the surface of a vertically oriented 50-mm diameter semiconductor wafer (Wafer World, West Palm Beach, FL), which was embedded in a Plexiglas plate fixed with a rigid rod to a dual-range force sensor (Vernier, Beaverton, OR). The gecko was pulled down an oxidized silicon (SiO_2, 100 orientation) or GaAs (type N-Si, 100 orientation) wafer until the toe slipped off. We measured shear force on the toes of the front and hind limbs. To measure only a single toe, we restrained the geckos by hand, and held the other toes in a flexed position. We excluded any trial in which the gecko struggled or moved its toe. However, the geckos proved incapable of releasing their toes while under high shear loads during a trial (approximately greater than 1 N). Thus, behavior of the live animal was unlikely to have affected values of maximal shear force of single toes. Real-time force data were collected on a computer (Power Macintosh, Apple with MACLAB CHART V3.6.5, ADInstruments, Sydney) at a rate of 40 Hz. Because force of adhesion is strongly correlated with pad area (27), we standardized the data by dividing the maximum force generated at each toe by the pad area of that toe to determine shear stress. We measured pad area for each gecko by scanning the animals on a flatbed scanner (Agfa) and analyzing the images with a commercial program (CANVAS 7.0.2, Deneba, Miami). We analyzed all data with a statistics program (STATVIEW 5.0.1; SAS Institute, Cary, NC).

Water droplet contact angle measurements. Water droplet contact angles were measured on isolated seta-bearing toe pads (scansors). We carefully peeled outer epidermal layer of single scansors from five restrained, nonmolting geckos. The scansors were affixed to glass slides, setal side up, using cyanoacrylate gel glue. The fixed scansors were oriented such that the setae formed a flat surface on which water contact angles could be measured under a microscope (Nikon SMZ-1500). Images (2,048 × 1,536 pixels) of ≈500-μm deionized droplets were captured on a digital camera (Nikon Coolpix 990). Water contact angles on the setal surface were measured in CANVAS 8 (Deneba) on a Macintosh computer.

Setal Adhesion. *Fabrication of MEMS cantilevers.* We used a (111) SIMOX SOI (silicon-on-insulator) wafer as the starting material, and defined cantilever patterns by contact lithography followed by plasma etching (28). The backside of the cantilevers were then patterned, again using contact lithography, and released using a DRIE (deep reactive ion etching) process. The buried oxide layer was removed in hydrofluoric acid, leaving a released cantilever. Silicon forms a thin native oxide layer on its surface when exposed to humid air. This silicon dioxide layer is hydrophilic. The "hydrophilic" data were taken while the cantilevers were covered in this thin layer of native oxide (θ = 0.0°). To produce a hydrophobic surface on the MEMS sensor, we used a vapor-phase hydrofluoric (HF) acid etch. HF removes the native oxide layer and produces a hydrogen-terminated silicon surface. The (111) surface of silicon can be passivated this way to prevent further oxidation for days. In the absence of a native oxide layer, the silicon surface is hydrophobic (θ = 81.9°). The "hydrophobic" data were taken within minutes of this chemical passivation. Because length, width, and thickness of the cantilever can be defined/measured precisely, and because the cantilever is made entirely of single crystal silicon, published mechanical properties of silicon (29) were used for force calibration.

Adhesion measurements on hydrophobic and hydrophilic MEMS sensors. We carefully peeled the outer epidermal layer of a single seta-bearing toe pad (scansor) off the toe of a restrained, live, nonmolting gecko. With the tip of a finely etched tungsten pin, we scraped the epidermal surface to break off individual setae at the base of the stalk. The isolated seta was then glued to the end of a no. 2 insect pin with 5-Minute epoxy (TTWDevcon, Danvars, MA). The pin had a tip diameter of approximately 15 μm. To prevent the epoxy from creeping up the stalk of the seta, which might change the mechanical property of the specimen, we precured the epoxy for ≈1 min before applying it to the specimen. The seta was oriented such that the spatular surface was approximately perpendicular to the axis of the pin. All preparations were completed under a compound microscope. The pin was then mounted on a computer-controlled piezoelectric actuator with closed-loop feedback using capacitive position sensors (Physik Instrument E-500.00, Karlsruhe, Germany). The actuator moved the spatular surface of the seta into contact with the cantilever and then pulled away at 10 μm/s. The experiments

Downloaded from https://www.pnas.org by CENTRAL SOUTH UNIVERSITY on November 9, 2026 from IP address 218.76.28.177.

were recorded on VHS videotape using a charge coupled device (CCD) camera (Sony CCD-IRIS). Deflections of the cantilever were measured by using captured images at the instant of detachment. Resolution was ± 0.4 μN, limited by the resolution of the video recording equipment.

Physical Model Adhesion. *Fabrication of synthetic setal tips.* We fabricated synthetic spatulae from two different hydrophobic (θ = 87°) polymer materials, silicone rubber (PDMS, polydimethylsiloxane; Dow–Corning, HS II) and polyester resin (TAP Plastics, Dublin, CA). Young's moduli of polymers were 0.57 MPa for the HS II and 0.85 GPa for the polyester, determined by measuring the stiffness of molded rectangular polymer beams of a known size. Synthetic spatulae were fabricated in dimensions similar to natural Tokay gecko spatulae (0.2 μm; ref. 30) using an Atomic Force Microscope (AFM)-based nanomolding technique. A flat wax surface (J. Freeman, Inc., Dorchester, MA) was punched with an AFM probe (Nanosensors, Wetzlar-Blankenfeld, Germany, Pointprobe cantilever with 42 N/m stiffness) with a conical tip of apex radius 10–20 nm and 15 μm height. The punched surface was then filled with polymer. After curing, molded polymer surfaces were detached from the wax by peeling.

Adhesion measurements for synthetic setal tips. Perpendicular adhesion force of the fabricated spatulae was measured by a rectangular tipless AFM probe. We used a laser micromachining system (QuickLaze-50; New Wave Research, Fremont, CA) to cut the tip end of a standard rectangular AFM probe (Nanosensors). After calibrating the probe stiffness, perpendicular force between the probe and the synthetic spatula was measured. There is ≈30% uncertainty in the synthetic spatulae contact radii estimates because of the AFM imaging and tipless probe contact location and orientation errors during the pull-off measurements. The rms surface roughness of PDMS and polyester were measured by AFM as ≈3 nm and 5 nm, respectively; thus, the roughness effect can be neglected. Measurements were made at 25°C and 58% relative humidity. Perpendicular forces were measured by using a probe with 1.75 N/m stiffness and 390 nm/s retraction speed.

Results and Discussion

Experimental Support of van der Waals Adhesion Hypothesis. The capillary adhesion hypothesis predicts high attachment forces on hydrophilic semiconductors (SiO_2) and low attachment forces on hydrophobic semiconductors (GaAs and Si). The van der Waals hypothesis predicts high attachment forces on all semiconductors, regardless of hydrophobicity. Our present measurements of live gecko toes and single setae on hydrophilic and hydrophobic semiconductor surfaces (Fig. 1) support the van der Waals hypothesis and reject the hypothesis that capillary adhesion determines adhesive force. Our results also reject the hypothesis that water contact angle (θ) of a surface predicts attachment forces in gecko setae, as suggested by prior studies (24, 25, 31). Parallel stress of live gecko toes on GaAs (0.213 N/mm^2 ± 0.007; $\bar{x}$ ± SE; n = 39) and Si (0.218 N/mm^2 ±0.008; $\bar{x}$ ± SE; n = 49) semiconductors was not significantly different (t = −0.463; df = 86; $P > 0.5$; Fig. 2). Adhesion of a single gecko seta on the hydrophobic MEMS cantilever (41.3 μN ± 0.18; $\bar{x}$ ± SE; n = 61) differed by only 2% from that measured on the hydrophilic sensor (40.4 μN ± 0.13; $\bar{x}$ ± SE; n = 70), and was similar to prior measurements using a dual-axis piezoresistive MEMS sensor (3, 32). Strong adhesion between two hydrophobic surfaces in air, such as adhesion of hydrophobic setae to the hydrophobic GaAs and Si MEMS surfaces, demonstrates that the mechanism of adhesion is van der Waals dispersion force (23).

To account for the high degree of similarity in adhesive forces measured on surfaces with somewhat different polarizabilities, consider that when van der Waals interactions occur between nonviscous bodies, under equilibrium conditions, adhesion will increase with an increase in the dielectric constant, ε, (and index of refraction, n) of one or both surfaces in approximate proportion to $(\varepsilon - 1)/(\varepsilon + 1)$ (23). Thus, over 66% of the increase in van der Waals force occurs over $1 < \varepsilon < 5$, and there is only a small increase in van der Waals force for increases in ε above 5. This may explain why we measured equivalent adhesion on highly polarizable surfaces (GaAs, ε = 10.88 and Si, ε = 11.8), and on moderately polarizable surfaces (SiO_2, $\varepsilon > 4.5$). Another interesting possibility is that maximum setal adhesion may not be limited by the strength of van der Waals bonds, but instead by failure of the keratin they are made of.



Fig. 2. Tokay gecko (*Gekko gecko*) adhering to molecularly smooth hydrophobic GaAs semiconductor. The strong adhesion between the hydrophobic surface of the gecko's toes and the hydrophobic GaAs surfaces demonstrates that the mechanism of adhesion in geckos is van der Waals force.

We found that gecko setae are strongly hydrophobic, as predicted for β-keratin structures (33–35). The water contact angle (θ) of gecko setae was 160.9° ± 1.4 SD; n = 5. The unusually large contact angle is likely to be caused by the micro-roughness of the seta and skin (36, 37), as has been discovered for the lotus plant (38). The hydrophobic nature of the seta supports the van der Waals hypothesis, and is inconsistent with the hypothesis that capillary adhesion determines adhesive force (24, 25, 31). In fact, high setal hydrophobicity may aid in decreasing the setal–substrate gap distance by excluding layers of water at points of contact, further reducing the role of capillary adhesion and increasing van der Waals forces.

van der Waals Model Predicts Actual Spatular Dimensions. If van der Waals adhesion determines setal force, then geometry and not surface chemistry should dictate the design of setae. Let us represent an individual seta as a stalk with a bundle of terminal tips (spatulae). If we model spatulae as cylinders, each with a hemispherical end of radius R adhering to a surface, then given our empirical measurements of adhesive force, we can apply a useful theory of adhesion (Johnson–Kendall–Roberts; refs. 4 and 23) to predict R for the spatulae. We measured ≈40 μN adhesion per seta on MEMS surfaces. There are ≈3,600 tetrads of setae per mm^2 (39), or 14,400 setae per mm^2. Therefore, adhesive stress from our force measurements is ≈576,000 N/m^2 (5.68 atmospheres; 1 atm = 101.3 kPa). The Johnson–Kendall–Roberts theory adhesion force for a sphere-plane model is $F = 3/2\pi RW$ per sphere (spatula in our case). If the spatulae are tightly packed together, the stress will be approximately $(3/2)\pi RW/\pi R^2 = (3/2)W/R$. Using a typical adhesion energy for van der Waals surfaces (W = 50–60 mJ/m^2), we can calculate the

Downloaded from https://www.pnas.org by CENTRAL SOUTH UNIVERSITY on November 9, 2026 from IP address 218.76.28.177.

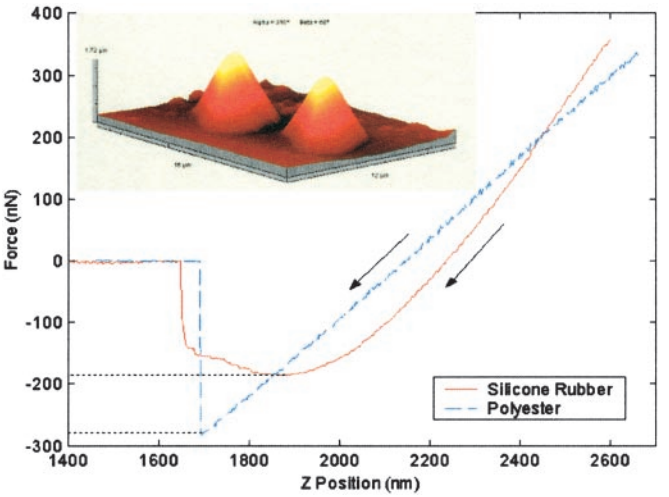


Fig. 3. Synthetic gecko spatulae and perpendicular pull-off force measurements using a tipless AFM probe. Sample synthetic PDMS spatulae are shown in the *Upper Left* AFM tapping mode image of $16 \times 12 \times 1.72$ μm^3 scan area. Adhesive function of the synthetic was similar to that of natural gecko setae, suggesting that specific surface chemistry is not required, and that an array of small, simple structures can be an effective adhesive.

predicted radii (R) of individual spatulae in the bundle using our force measurements: $R = (3/2)W^*$ area$/F = 0.13$–0.16 μm. This value is close to empirical measurements (3, 5). Even though the calculation is only a gross approximation, it shows that our measurements are quantitatively consistent with a van der Waals dispersion interaction between setae and substrates. It predicts that for a given thermodynamic adhesion energy, smaller spatulae will result in a greater adhesive force per unit area. This finding may not only assist us in explaining the function of setal structures in animals, but also suggests that synthetic adhesives could be enhanced simply by subdividing their surface into small protrusions to increase surface density.

Spatular Physical Model Supports van der Waals Adhesion Hypothesis. Perpendicular force was 181 ± 9 nN ($n = 25$) for PDMS spatulae with tip radius of 230–440 nm (Fig. 3) and 294 ± 21 nN ($n = 20$) for polyester spatulae with tip radius of ≈350 nm. We can estimate the van der Waals contribution to the adhesive forces of our synthetic spatulae: $F_{vdw} = HR/6d_0^2$, where $d_0 \approx 0.165$ nm (23) is the cutoff distance and H is the Hamaker constant. Using $H \approx 45 \times 10^{-21}$ J [estimated from $H \approx 2.1 \times 10^{-21}\gamma$ (mJ/m2); ref. 23] for PDMS, $H = 60.9 \times 10^{-21}$ J (40) for polyester, and $H = 68.4 \times 10^{-21}$ J (40) for SiO_2, $F_{vdw} = 114$ nN and $F_{vdw} = 139$ nN are predicted for PDMS and polyester, respectively. Conservatively, 47–63% of the adhesion forces of the synthetic spatulae can be explained by van der Waals forces, suggesting that our synthetic spatulae approximate the function of natural spatulae. Johnson–Kendall–Roberts adhesion theory predicts an adhesive force $F = 3/2\pi RW$, where $W = \sqrt{\gamma_1\gamma_2}$, and $\gamma_1 = 115$–200 mJ/m^2 (41) and γ_2 are the surface energies of the SiO_2 layer of the silicon probe and the polymer, respectively. Predicted perpendicular forces for PDMS using the Johnson–Kendall–Roberts model (185 nN, for $\gamma_2 = 21.4$ mJ/m^2; ref. 42; $R \approx 335$ nm) and polyester (280 nN, for $\gamma_2 = 44.6$ mJ/m^2; ref. 42) were within error bounds of measured values, providing further support that our synthetic spatulae approximate the structure and function of natural spatulae.

The use of van der Waals dispersion force by geckos suggests that evolution can result in an effective adhesive by simply building an array of small structures rather than by synthesizing a structure with a specialized surface chemistry. Thus, geckos have been able to exploit the peculiarities of their epidermal structure (5, 35, 36) and evolve elaborate microstructures with phenomenal adhesive properties. Maximizing surface density as predicted by the Johnson–Kendall–Roberts model may represent the most important design principle underlying the multiple convergent evolutions of keratinous setae in geckos (43–46), and in convergent adhesive systems in anoles (47), and skinks (30). Interestingly, insects too have evolved adhesive setae (2, 6, 7, 10, 12, 13, 21, 48–60) using a different material, chitin. This is a further indication that geometry, not surface chemistry, is the central design principle in the evolution of adhesive setae.

Our preliminary physical models provide proof of concept that humans can fabricate the first dry, adhesive microstructures when inspired by biology. There is a striking contrast between the simple Johnson–Kendall–Roberts-based models we used and the geometrically complex structures evolved by geckos. Each Tokay seta bears hundreds of tips on a curved shaft, and the tips themselves consist of a stalk with a thin, roughly triangular end, where the apex of the triangle connects the tip to its stalk. It is likely that the added complexity of gecko setae provides ease of attachment and detachment (3), and the ability to adhere to rough as well as smooth surfaces. We find it remarkable, however, that the geometrically simple Johnson–Kendall–Roberts model and our physical models were sufficient to approximate the function of setal tips. We suggest that development of biologically inspired dry adhesive microstructures will not require direct biomimicry of complex gecko setal structures, but rather application by analogy of the essential design principles underlying their evolution.

We thank S. Attinasi, S. Autumn, W. Federle, G. Hermann, S. McGonagle, A. Russell, and three anonymous referees. This work was supported by Defense Advanced Research Projects Agency Grants N66001-00-C-8047 and N66001-01-C-8072 from the Controlled Biological and Biomimetic Systems Program, Defense Sciences Office, under the auspices of Dr. Alan Rudolph (to K.A., R.J.F., R.F., and T.K.).

1. Aristotle, *Historia Animalium*, trans. Thompson, D. A. W. (1918) (Clarendon, Oxford), http://classics.mit.edu/Aristotle/history_anim.html.
2. Stork, N. E. (1980) *J. Exp. Biol.* **88,** 91–107.
3. Autumn, K., Liang, Y. A., Hsieh, S. T., Zesch, W., Chan, W.-P., Kenny, W. T., Fearing, R. & Full, R. J. (2000) *Nature (London)* **405,** 681–685.
4. Johnson, K. L., Kendall, K. & Roberts, A. D. (1973) *Proc. R. Soc. London Ser. A* **324,** 310–313.
5. Ruibal, R. & Ernst, V. (1965) *J. Morphol.* **117,** 271–294.
6. Edwards, J. S. & Tarkanian, M. (1970) *Proc. R. Entomol. Soc. London* **45,** 1–5.
7. Gillett, J. D. & Wigglesworth, V. B. (1932) *Proc. R. Soc. London Ser. B* **111,** 364–376.
8. Lees, A. D. & Hardie, J. (1988) *J. Exp. Biol.* **136,** 209–228.
9. Federle, W., Brainerd, E. L., McMahon, T. A. & Hölldobler, B. (2001) *Proc. Natl. Acad. Sci. USA* **98,** 6215–6220.
10. Eisner, T. & Aneshansley, D. J. (2000) *Proc. Natl. Acad. Sci. USA* **97,** 6568–6573.
11. Jiao, Y., Gorb, S. & Scherge, M. (2000) *J. Exp. Biol.* **203,** 1887–1895.
12. Gorb, S. N. (1998) *Proc. R. Soc. London B* **265,** 747–752.
13. Walker, G., Yule, A. B. & Ratcliffe, J. (1985) *J. Zool. (London)* **205,** 297–307.
14. Emerson, S. B. & Diehl, D. (1980) *Biol. J. Linn. Soc.* **13,** 199–216.
15. Green, D. M. (1981) *Copeia* **4,** 790–796.
16. Hanna, G. & Barnes, W. J. P. (1991) *J. Exp. Biol.* **155,** 103–125.
17. Rosenberg, H. I. & Rose, R. (1999) *Can. J. Zool.* **77,** 233–248.
18. Bellairs, A. (1970) *The Life of Reptiles* (Universe Books, New York).
19. Mahendra, B. C. (1941) *Proc. Indian Acad. Sci. Sect. B* **13,** 288–306.
20. Dellit, W.-D. (1934) *Jena. Z. Naturw.* **68,** 613–656.
21. Scherge, M. & Gorb, S. N. (2001) *Biological Micro- and Nanotribology: Nature's Solutions* (Springer, Berlin).
22. Baier, R. E., Shafrin, E. G. & Zisman, W. A. (1968) *Science* **162,** 1360–1368.
23. Israelachvili, J. (1992) *Intermolecular and Surface Forces* (Academic, New York).
24. Hiller, U. (1969) *Forma et functio* **1,** 350–352.
25. Hiller, U. (1968) *Z. Morph. Tiere* **62,** 307–362.
26. Blakemore, J. S. (1982) *J. Appl. Phys.* **53,** R123–R181.

Downloaded from https://www.pnas.org by CENTRAL SOUTH UNIVERSITY on November 9, 2026 from IP address 218.76.28.177.

27. Irschick, D. J., Austin, C. C., Petren, K., Fisher, R., Losos, J. B. & Ellers, O. (1996) *Biol. J. Linn. Soc.* **59,** 21–35.
28. Chui, B. W., Kenny, T. W., Mamin, H. J., Terris, B. D. & Rugar, D. (1998) *Appl. Phys. Lett.* **72,** 1388–1390.
29. Petersen, K. E. (1982) *Proc. IEEE* **70,** 420–457.
30. Williams, E. E. & Peterson, J. A. (1982) *Science* **215,** 1509–1511.
31. Hiller, U. (1975) *J. Bombay Nat. Hist. Soc.* **73,** 278–282.
32. Liang, Y. A., Autumn, K., Hsieh, S. T., Zesch, W., Chan, W.-P., Fearing, R., Full, R. J. & Kenny, T. W. (2000) in *Technical Digest of the 2000 Solid-State Sensor and Actuator Workshop*, *Hilton Head Island, SC* (Transducers Research Foundation, Cleveland).
33. Bereiter-Hahn, J., Matoltsy, A. G. & Richards, K. S. (1984) *Biology of the Integument 2: Vertebrates* (Springer, New York).
34. Wainwright, S. A., Biggs, W. D., Currey, J. D. & Gosline, J. M. (1982) *Mechanical Design in Organisms* (Princeton Univ. Press, Princeton).
35. Russell, A. P. (1986) *Can. J. Zool.* **64,** 948–955.
36. Maderson, P. F. A. (1964) *Nature (London)* **203,** 780–781.
37. Stewart, G. & Daniel, R. (1972) *Copeia* **1972,** 252–257.
38. Barthlott, W. & Neinhuis, C. (1997) *Planta* **202,** 1–8.
39. Schleich, H. H. & Kästle, W. (1986) *Amphibia-Reptilia* **7,** 141–166.
40. French, R. H. (2000) *J. Am. Ceram. Soc.* **83,** 2127–2146.
41. Yu, M., Kowalewski, T. & Ruoff, R. S. (2000) *Phys. Rev. Lett.* **86,** 87–90.
42. Li, L., Mangipudi, V. S., Tirrell, M. & Pocius, A. V. (2001) in *Fundamentals of Tribology and Bridging the Gap Between the Macro- and Micro/Nanoscales* (Kluwer Academic, Dordrecht, The Netherlands), pp. 305–329.
43. Russell, A. P. (1972) Ph.D. dissertation (Univ. of London).
44. Russell, A. P. (1976) in *Morphology and Biology of Reptiles*, eds. Bellairs, A. D. & Cox, C. B. (Academic, London), pp. 217–244.
45. Russell, A. P. (1979) *Copeia* **1979,** 1–21.
46. Bauer, A. M. & Russell, A. P. (1990) *Mem. Queensl. Mus.* **29,** 299–310.
47. Peterson, J. A. & Williams, E. E. (1981) *Bull. Mus. Comp. Oology* **149,** 215–268.
48. Nachtigall, W. (1974) *Biological Mechanisms of Attachment: The Comparative Morphology and Bioengineering of Organs for Linkage, Suction, and Adhesion* (Springer, New York).
49. Bauchhenss, E. & Renner, M. (1977) *Int. J. Insect Morphol. Embryol.* **6,** 225–227.
50. Hill, D. E. (1977) *Zool. J. Linn. Soc.* **60,** 319–338.
51. Rovner, J. S. (1978) *Symp. Zool. Soc. London* **42,** 99–108.
52. Stork, N. E. (1983) *J. Nat. Hist.* **17,** 829–835.
53. Wigglesworth, V. B. (1987) *J. Exp. Biol.* **129,** 373–376.
54. Roscoe, D. T. & Walker, G. (1991) *Bull. Br. Arachnol. Soc.* **8,** 224–226.
55. Betz, O. (1996) *Zoomorphology* **116,** 15–34.
56. Attygalle, A. B., Aneshansley, D. J., Meinwald, J. & Eisner, T. (2000) *Zoology (Jena)* **103,** 1–6.
57. Koelsch, G. (2000) *Can. J. Zool.* **78,** 465–475.
58. Gorb, S., Gorb, E. & Kastner, V. (2001) *J. Exp. Biol.* **204,** 1421–1431.
59. Gorb, S. N. & Beutel, R. G. (2001) *Naturwissenschaften* **88,** 530–534.
60. Gorb, S. N. (2001) *Attachment Devices of Insect Cuticle* (Kluwer Academic, Dordrecht, The Netherlands).

Downloaded from https://www.pnas.org by CENTRAL SOUTH UNIVERSITY on November 9, 2026 from IP address 218.76.28.177.